Fabian Roos, Jonathan Bechter, Christina Knill,
Benedikt Schweizer, and Christian Waldschmidt

Radar Sensors for Autonomous Driving

Autonomous driving is currently the focus of considerable media attention, and the automotive industry is working on harnessing technological advances to acceler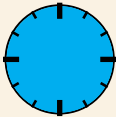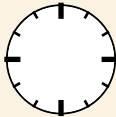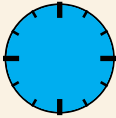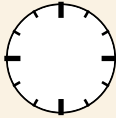ate development. In doing so, different levels of automated driving must be mastered (Table 1) and defined [1]. At higher automation levels, the execution, monitoring, and fallback performance are increasingly handled by the system and not the human driver, resulting in more demanding requirements for
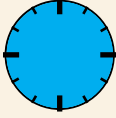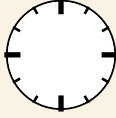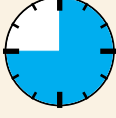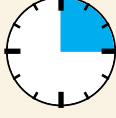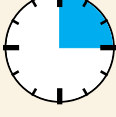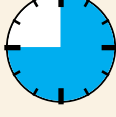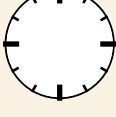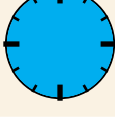
Fabian Roos (roos@ieee.org), Jonathan Bechter (jonathan.bechter@alumni.uni-ulm.de),
Christina Knill (christina.knill@uni-ulm.de), Benedikt Schweizer (benedikt.schweizer@uni-ulm.de), and Christian Waldschmidt
(Christian.Waldschmidt@uni-ulm.de) are with the Institute of Microwave Engineering, Ulm University, Germany.

TABLE 1. Levels of automated driving defined by [1]. The clock symbol indicates the portion of travel time handled by the human or by the system.

Society of Automotive Engineers Level	Human Tasks		System Tasks	
0 No automation		• Execution of steering, velocity control • Environmental perception		• None
1 Driver assistance		• Part of steering/velocity control • Observation of system • Environmental perception		• Part of steering/velocity control
2 Partial automation		• Observation of system • Environmental perception		• Execution of steering/velocity control
3 Conditional automation		• Interaction when requested		• Execution of steering/velocity control • Environment perception
4 High automation		• Human doesn't need to rapidly respond		• All driving mode-specific tasks handled by system • System goes in error case in a safe state
5 Full automation		• None		• Full-time performance under all roadway and environmental conditions

the sensor system. As shown in [2], radar sensors are a key technology to enable Society of Automotive Engineers level 5, full automation.

In contrast to video cameras and laser scanners, a radar sensor is almost completely unaffected by severe weather and light conditions, and it remains operational in complete darkness and snowfall. By exploiting the reflections of the electromagnetic waves between road surfaces and the underbody of vehicles, radar sensors can even detect hidden targets behind other vehicles.

Some Key Tasks To Advance Autonomous Driving

High-Resolution Capabilities: Enabling Advanced Driver-Assistance Functions

With a radar sensor, the radial distance, velocity, and angle of targets can be measured. Key parameters are the accuracy of the measurement and resolution, i.e., the ability to distinguish close targets. For certain driver-assistance functions, typically those identified by the Society of Automotive Engineers as level 1 (Table 1), it was sufficient that a radar sensor be able to distinguish different objects and estimate one scattering center (or a small
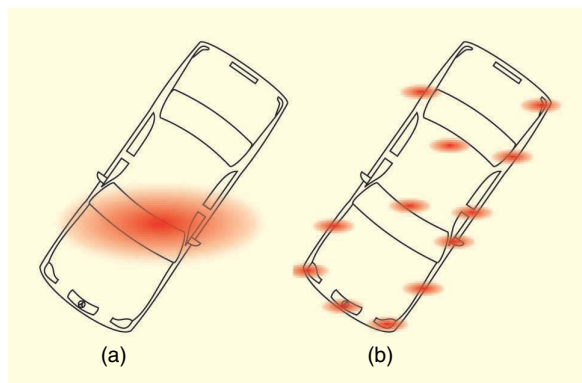
Figure 1. *(a) With a low-resolution sensor, an extended target vehicle is detected as a single-point target, because just one scattering center can be distinguished on the object (the red blurred ellipse). (b) Only by using high-resolution radar sensors can different scattering centers on a target vehicle be distinguished (the red blurred ellipses).*

number of scattering centers) per object, regardless of size [3] [Figure 1(a)]. However, a vehicle has many scattering centers because of its different curvatures, corners, and slots [4]–[6]. These scattering centers can be measured

using a high-resolution sensor [Figure 1(b)]. In the example shown in Figure 1(b), a higher angular resolution is necessary and can be achieved with a larger antenna aperture, as explained later in the article. Additionally, a high Doppler resolution is helpful to distinguish different
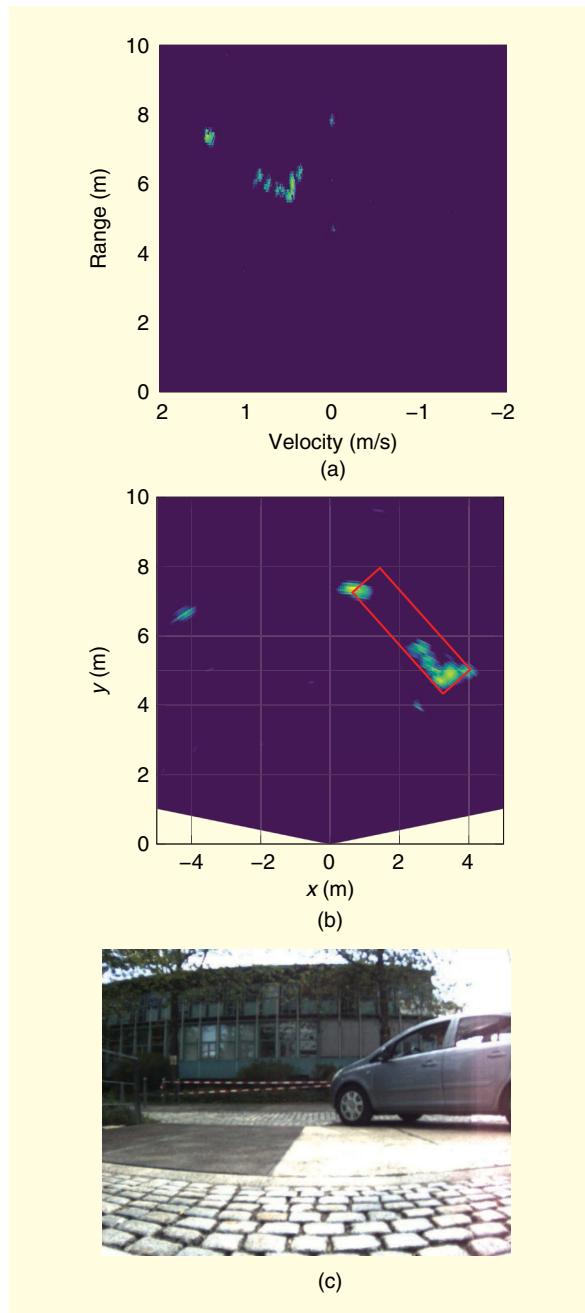
Figure 2. *Measuring a target vehicle with an experimental radar sensor. The measurements shown are from a top view, while the camera image is a side view. (a) The range-Doppler evaluation of the target vehicle. (b) The x-y representation of the target vehicle with estimated orientation (red box), as described in [15] and [16]. (c) A camera image of the measured scenario.*

radial velocities of the target. The modulation parameters must be adapted for a higher Doppler resolution (also described later). Signal processing algorithms can be also applied to achieve a higher resolution [7]–[9].

Current automotive radar sensors operate mainly in the 77–81-GHz frequency range and will continue to do so in the future because this part of the spectrum is defined by the International Telecommunication Union [10] for future automotive radar sensors. Furthermore, the European Union [11] and the United States [12] have already allocated this frequency band. European regulations—and, therefore, also German [13] regulations—specify a maximum radiated average power spectral density of −3 dBm/MHz inside and −9 dBm/MHz outside of the vehicle. For the United States, the limitation is given by a maximum equivalent isotropically radiated power (EIRP) of 50 dBm within this frequency band. Additionally, the European and American regulations specify a maximum peak power of 55-dBm EIRP. A second frequency band of around 24 GHz, which is currently being used, will not be available worldwide in the future because new vehicles using this frequency range will not be permitted after 2018 in, for example, Germany [14].

Figure 2 depicts an urban scenario, where a target vehicle is measured with an experimental radar sensor. In the range-Doppler evaluation of Figure 2(a), the moving object's velocity distribution can be seen. When an angle estimation is applied, the contour becomes visible [Figure 2(b)]. The video image in Figure 2(c) is used for validation purposes and shows the measured scene. As can be observed, the moving object is detected with several reflections.

Vehicle Maneuver Planning: Dimension, Orientation, and Motion State Estimation of Target Vehicles

The target vehicles' dimension, orientation, and motion state can be used by an autonomous vehicle to plan its driving maneuvers, and high-resolution radar sensors are able to extract dimension and orientation [15], [16], [Figure 2(b)]. Using orientation, it is possible to detect lane changes more quickly than with a conventional tracking filter because the filter usually needs several steps to predict motion correctly. With two radar sensors, it is even possible to estimate the complete motion state, e.g., the orientation and movement vector, including the yaw rate, of a target vehicle [17].

Vulnerable Road-User Detection and Classification: Micro-Doppler Analysis

Vulnerable road users, such as pedestrians and cyclists, must be detected and classified, especially in urban areas [18]. As the reflected power from such road users is much lower than that from vehicles, the radar

sensor must be sensitive to weak targets [19]. Due to the pedestrians' movement, various different Doppler velocities can be measured using the micro-Doppler effect [20] (Figure 3). In [21], the authors provide measurement results of such vulnerable road users with a high-resolution radar sensor.

Self-Localization: Ego Motion and Position Estimation Using Doppler Distribution of Radial Velocities and Grid Maps

For self-localization, the precise knowledge of the vehicle's own motion and position, also called *ego motion and position*, is important. The motion and position can be determined using radar sensors [22], [23] more robustly and with fewer errors compared to standard vehicle odometry during highly dynamic maneuvers [2]. Additionally, landmarks are often used for self-localization [2], [24] by recognizing prominent, strongly reflective objects in the environment.

Enabling 360° Environmental Perception: Multiradar Sensor Setup

To operate at the full automation level, a multiradar sensor setup is necessary [2], such as the one used in the autonomous vehicle Bertha [25] in Figure 4. With such a setup, 360° environmental perception is possible, which is necessary for crossings, roundabouts, and

overtaking maneuvers. The requirements for the radar sensors differ for urban and highway applications. Either the sensors can operate in different modes, such
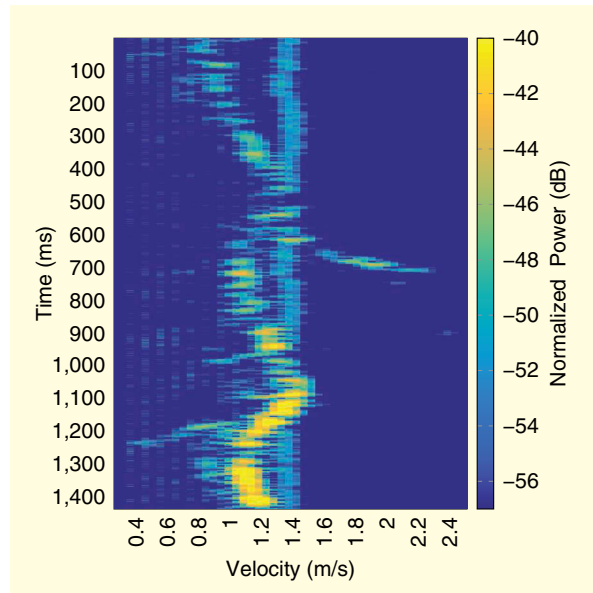
Figure 3. *A color graph showing velocity distribution of a walking pedestrian over time. The nearly constant velocity component is the main body part, while the changing parts correspond to the arms and legs.*
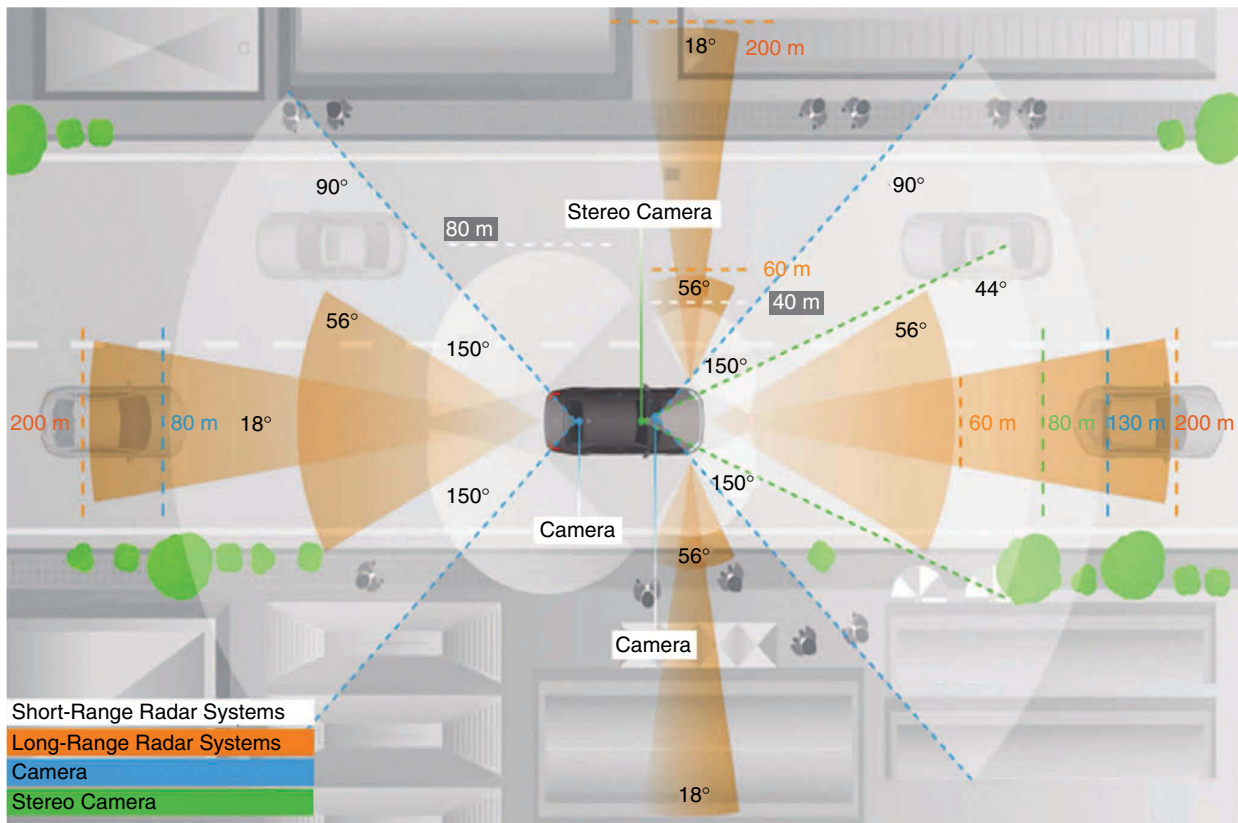
Figure 4. *The sensor setup for the autonomous vehicle Bertha. Image taken from [25].*

as long- and short-range mode, or different sensors are used. Usually, the mode of operation determines the maximum unambiguously covered distance and velocity and the corresponding field of view.

Robustness: Interference Mitigation

With high market penetration of radar sensors, the possibility of interference rises dramatically. For higher automation levels, permanent situation awareness is paramount, and sudden blindness, overlooking weak targets, or detecting ghost targets must be avoided at all times. Hence, possible harmful interference should, at least, be detected and, in the best case, mitigated. Therefore, different interference cases must be evaluated based upon the modulation formats used.

Mass Production: Demand for Low-Cost Hardware

To make it practical to equip nearly every vehicle with one or several radar sensors to achieve 360° coverage, each single sensor must be as inexpensive as possible. Therefore, the hardware requirements should be kept maximally basic, which means simple signal generation, a small number of analog-to-digital converters (ADCs), and sampling frequencies in the lower-megahertz range.

Figure 5 illustrates how to reduce these hardware requirements for direction-of-arrival (DoA) estimation. A better DoA estimation occurs if the aperture of the receiving antenna elements is large. A large aperture can be achieved with more receiving elements, as in the classic approach [Figure 5(a)]. Because every receiving element requires an ADC, the hardware effort increases as well as the required memory to store the sampled data.

Using a multiple-input, multiple-output (MIMO) radar setup, the aperture can be increased while maintaining fewer required ADCs. Usually, the number of transmitting elements is increased, and a reasonable number of receiving elements is chosen [Figure 5(b)]. If three transmitters and eight receiving elements are used, the virtual aperture consists of 24 elements. To operate a MIMO radar, orthogonal waveforms are necessary. Different algorithms are available to perform the DoA estimation based on the various received signals [26]. For example, the Bartlett beamformer, subspace methods [27], or maximum-likelihood approaches [28]. If the virtual antenna elements are equally spaced, the Bartlett beamformer can be interpreted as a simple Fourier transform. A performance comparison between different DoA algorithms as functions of the signal-to-noise ratio is given in [29].

To achieve high spatial resolution, the modulation format is a crucial element, as it dictates all further signal processing. An ideal modulation format should deliver high resolution, be able to detect and distinguish multiple targets, and make the lowest possible demands on hardware to enable low-cost mass production. As hardware improves, more powerful modulation formats can be anticipated. Smart signal processing of the modulation formats can additionally decrease the required hardware effort.

Automotive Radar Modulation Schemes

Most radars sensors [30] apply the state-of-the-art chirp-sequence modulation format, the successor of the well-known frequency-modulated continuous wave (FMCW) modulation format. With the ongoing development of faster ADCs, applying digital modulation formats, such as code modulation or orthogonal frequency-division multiplexing (OFDM), becomes feasible.

Often Used: FMCW With Slow Ramps

The key idea of the classic FMCW modulation scheme is to transmit linear frequency ramps with different slopes [Figure 6(a)]. The transmit time is usually in the range of a couple of milliseconds, and the number of transmitted ramps is limited. (This realization is also called *slow-ramp modulation*.) The transmit signal is reflected by a target, and the received signal is mixed with the transmit signal [31], [32]. After downconversion, each reflection from a target results in a sinusoidal signal component after mixing, which depends on the range to the target and the Doppler shift. If the bandwidth of the transmit signal typically is within the range of a gigahertz, the resulting baseband signal is in the range of several hundred kilohertz. Hence, the baseband signal can be sampled after an antialiasing low-pass filter with a slow, low-cost ADC.

The baseband signal, also called the *beat signal*, consists of the range and Doppler velocity of the target. To distinguish between the two components, different ramp slopes are required. To resolve multiple targets, the number of different ramp slopes must be increased accordingly [32].
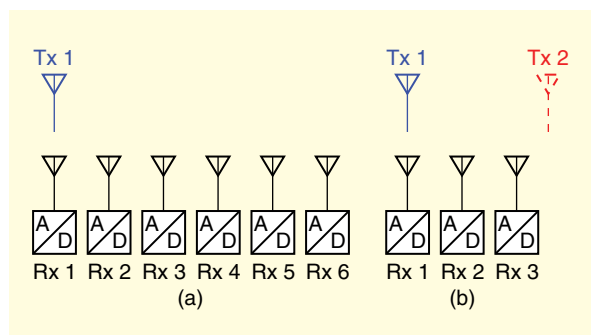

Figure 5. *A comparison of (a) a classic single-input, multiple output (SIMO) case using one transmitter (Tx) and six receivers (Rxs) with (b) the corresponding MIMO realization, resulting in the same virtual aperture size. With the MIMO realization using two transmit antennas, the number of receivers and therefore the number of ADCs (boxes labeled A/D) can be reduced.*

Challenging Task in Automotive Environments: Multitarget Scenarios

The typical automotive environment consists of multiple targets, which must be discriminated. With the classic FMCW scheme and a reasonable number of different ramp slopes, only a limited number of targets can be distinguished in a single measurement. Usually, there are more targets present than can be detected unambiguously. This can be solved either by tracking targets over time or with the following fast-ramp modulation scheme.

State of the Art: Fast Ramps/ Chirp-Sequence Modulation

In the slow-ramp procedure, the baseband signal depends on the range and the Doppler. If a single frequency ramp is steep [Figure 6(b)], the range-dependent part dominates the baseband signal, and the Doppler dependency can be neglected for a single ramp [32], [33]. Thus, the Doppler estimation requires a sequence of frequency chirps, which is why this modulation format is called *fast ramps* or *chirp-sequence modulation*. As the range and Doppler information is separated, a two-dimensional Fourier transform can be used for evaluation.

The advantage of fast-ramp modulation over the slow-ramp procedure is that the former is capable of distinguishing multiple targets in a single measurement. A drawback of the steeper ramps, however, is that the resulting baseband frequencies are typically in the range of several megahertz, which increases the sampling effort.

Influence of Key Modulation Parameters

The key parameters of chirp-sequence modulation are depicted in Figure 7 and listed in Table 2. The bandwidth B is directly linked to the range resolution ΔR, while the chirp repetition time T_r influences the unambiguously detectable Doppler frequency v_{max}. The sampling frequency f_s limits the maximum range. The total measurement time $T = LT_r$ affects the achievable Doppler resolution Δv [34]. The time between two consecutive measurements T_b is the update rate and is important in a fast-changing environment. The similarity to the slow FMCW modulation scheme can be seen in the comparison of parameter dependencies in Table 3.

Enhancing Unambiguous Doppler Velocity

Aliasing effects due to undersampling in the range domain can be removed through a low-pass filter before the analog-to-digital conversion. Fast-moving targets can cause ambiguities because the Doppler domain cannot be filtered. Therefore, the unambiguous velocity
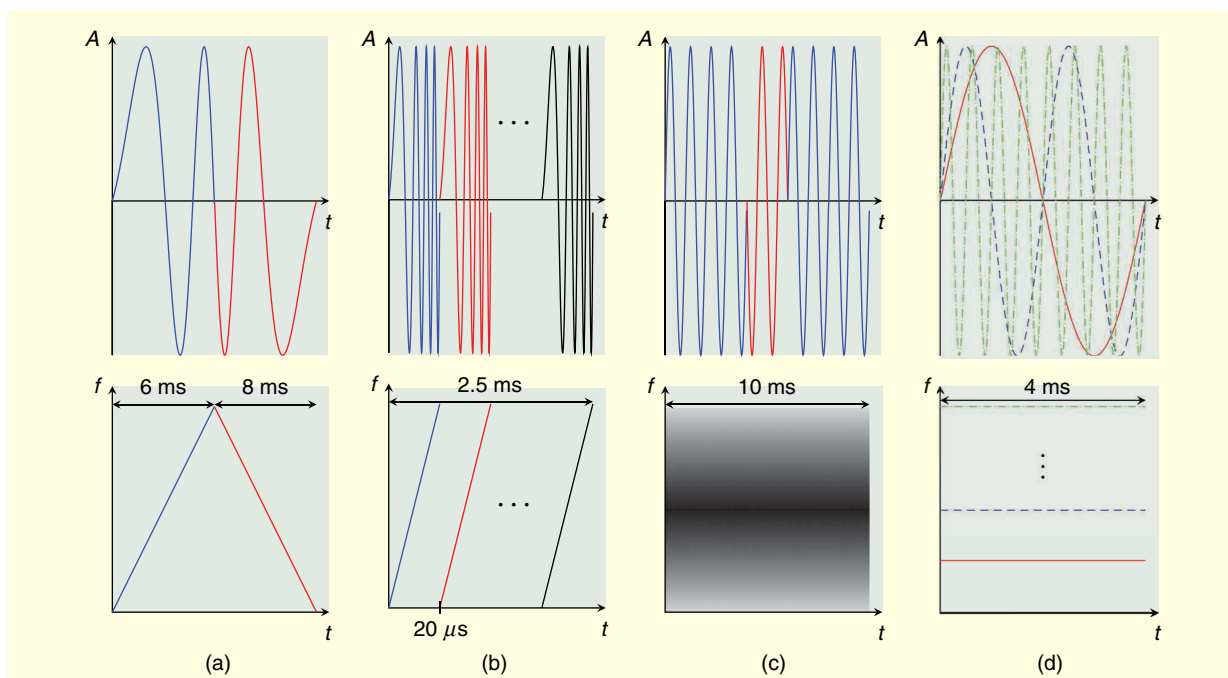
Figure 6. *An overview of different modulation formats in the time domain (top) and frequency domain (bottom). (a) The FMCW format usually transmits ramps with different slopes; depicted are an up (blue) and a down (red) ramp. (b) The chirp-sequence format uses, in this example, a sequence of 128 different frequency chirps (plotted in a different color) with a short duration. The pseudonoise modulation format in (c) switches the carrier rapidly with binary phase-shift -keying modulation (color indicates the phase code). The corresponding spectrum shows the applied window function, in this case a Hann window. (d) OFDM uses several orthogonal subcarriers (each shown in a different color), which carry the encoded information. The whole spectrum is used. A: amplitude; t: time; f: frequency.*

should be as large as required for the respective application. To detect high Doppler velocities, either the chirp repetition time must be reduced, or the modulation format must be adapted. Faster frequency ramps are more challenging to generate linearly and increase the sampling effort because the frequency of the resulting beat signal is increased.

One way to adapt the modulation format is to alter the repetition times in consecutive measurements and apply the Chinese remainder theorem [33]. Other authors suggest adapting the modulation format using the interlaced chirp-sequence approach, as presented in [35], [36]. The

Figure 7. *A graph showing the key modulation parameters of the state-of-the-art chirp-sequence modulation scheme.*

TABLE 2. The parameter dependencies of chirp-sequence modulation.

Parameter	Dependency
ΔR	$\approx \dfrac{c}{2B}$
Δv	$= \dfrac{c}{2f_c L T_r} = \dfrac{c}{2f_c T}$
R_{max}	$= \dfrac{c T_c}{4B} f_s$
v_{max}	$= \dfrac{c}{4f_c T_r}$
ADC rate	≤ 10 MHz (typical)

c: speed of light; f_c: carrier frequency; T_r: ramp repetition time; R_{max}; maximal unambiguous range.
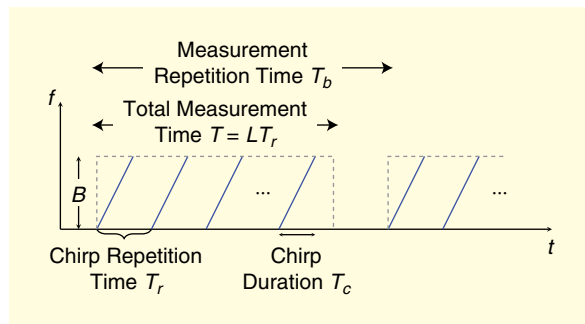
TABLE 3. The parameter dependencies of slow-ramp modulation.

Parameter	Dependency
ΔR	$\approx \dfrac{c}{2B}$
Δv	$= \dfrac{c}{2f_c T}$
R_{max}	$= \dfrac{cT}{2B}\left(\dfrac{f_s}{2} - \dfrac{2f_c v_{max}}{c}\right)$
v_{max}	$= \dfrac{c}{2f_c}\left(\dfrac{f_s}{2} - \dfrac{2B R_{max}}{cT}\right)$
ADC rate	≤ 1MHz (typical)

basic idea is that consecutive frequency ramps have increasing center frequencies. Sampling points of different frequency ramps can then be evaluated as a resulting long frequency ramp with fast repetition rates to enhance the unambiguous Doppler domain.

Increasing Angular Resolution: Application of MIMO

As mentioned in the "Mass Production: Demand for Low-Cost Hardware" section, orthogonal waveforms are required to associate different signals with their corresponding transmitters. As presented in [37] and [38], for chirp-sequence radars, time-, frequency-, or code-division multiplexing is typically used. For time-division multiplexing, the different transmitters are active one after another. As time passes between the consecutive measurements of the transmit antennas, the angular phase information is corrupted by Doppler shifts from moving targets. This error is usually either neglected for slow velocities or compensated for by a double or overlapping element in the virtual aperture [39]. In [40], it is shown that such an overlapping element is not required and that the motion compensation can be resolved with smart signal processing. For frequency-division multiplexing, the transmit antennas are active at the same time but at different center frequencies. Each target is therefore detected at different beat frequencies. Code-division multiplexing exploits orthogonal codes. Each transmit signal is encoded by a unique orthogonal code and recovered at the receiver [41].

A Code-Modulated Approach: Phase-Modulated CW Radar

Code-modulated radars [spread spectrum, pseudo-noise (PN), and phase-modulated continuous wave (CW)] transmit a wide-band code sequence modulated on a high-frequency CW carrier signal [Figure 6(c)]. On the receiver side, the signals are downconverted and correlated with the transmitted code sequence (Figure 8). The codes have a short duration T_{s2s}, such that the Doppler effect does not influence the correlation. Peaks in the correlation yield the time of flight and thus the object distance. A PN radar transmits a series of code sequences for Doppler extraction, as the phase of the CW carrier changes between the transmitted sequences. A Fourier transform across all transmitted sequences yields the velocity information; however, in contrast to chirp-sequence radars, PN radars require an in-phase quadrature (I-Q) receiver to distinguish positive and negative velocities. A proper selection of the code offers low-range side lobes or a low cross correlation with other codes [42]. The parameter dependencies summarized in Table 4 are very similar to the parameter dependencies of chirp-sequence radars.

An important aspect of PN radars is realizing the correlation of the receive signal. A correlation is possible in
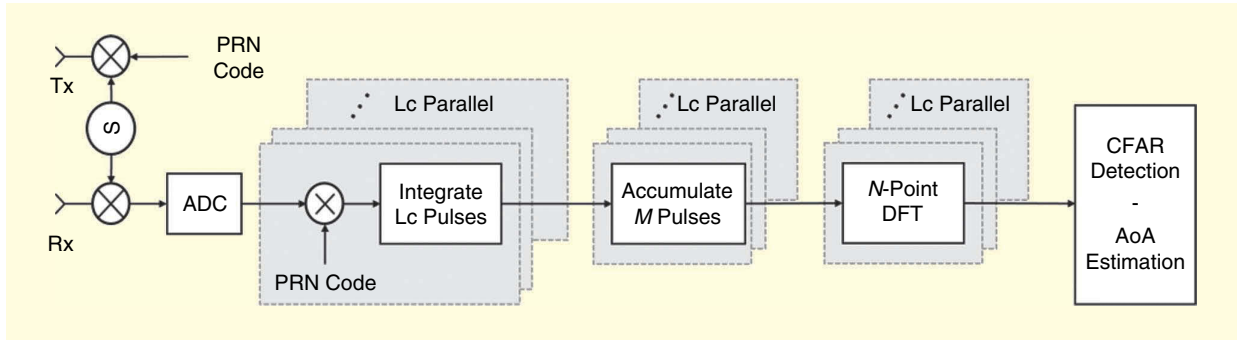
Figure 8. *A schematic of a code-modulated radar with fully digital processing. Figure taken from [43]. DFT: discrete Fourier transform; PRN: pseudo-random noise; Lc: length of code sequence; CFAR: constant false alarm rate; AoA: angle of arrival.*

the digital domain after sampling the receive signal [44]; however, this requires a very high sampling rate, as the baseband bandwidth is equal to the RF modulation bandwidth. Consequently, high data rates must be handled. Such systems for the 79-GHz band with bandwidths up to 2 GHz and a focus on automotive applications are discussed in [45]–[47]. The high sampling rate leads to a large integration gain. The authors of [48] use this fact to reduce the ADC resolution to only 4 b, which reduces the data rate significantly. They show that their sensor is still able to detect pedestrians at a distance of 30 m. The correlation can also be done in the analog domain with time-delayed versions of the code sequence for all range cells, one after another [49]–[52]. This offers reduced effort in signal processing but leads to a high measurement time when many different range cells are measured. Many parallel correlators can compensate for this increase in measurement time, but they lead to more hardware effort.

The application of orthogonal codes for multiple transmitters allows multiple sensors to operate at the same time in the same frequency band without undesired interactions. Such a time- and frequency-parallel MIMO system without the need for multiplexing is presented in [43] and [53].

A Digital Modulation Format: OFDM

Progress in digital technology over the past few years has encouraged approaches that shift the major effort of radar systems to the digital domain. Such systems, instantiated as software-defined radio (SDR), provide capabilities that are hard to match with common single-carrier radars. These capabilities include unmatched flexibility, adaptivity, robustness, ample calibration opportunities, and efficient channel usage.

A multicarrier modulation scheme suitable for an SDR and radar detection is OFDM (Table 5), which is also widely used in communication technology [54]. OFDM dates back to the 1960s [55], [56], but did not attract attention for radar applications until the last decade. The idea of a multicarrier radar scheme was first brought up by Levanon [57] in 2000. Driven by the

TABLE 4. The parameter dependencies of code-modulated radars.

Parameter	Dependency
ΔR	$\approx \dfrac{c}{2B}$
Δv	$= \dfrac{c}{2f_c L T_{s2s}} = \dfrac{c}{2f_c T}$
R_{max}	$= \dfrac{c T_{s2s}}{2}$
v_{max}	$= \dfrac{c}{4f_c T_{s2s}}$
ADC rate	$\leq 1\,\text{GHz}$ (typical, I and Q channel)

TABLE 5. The parameter dependencies of OFDM.

Parameter	Dependency
ΔR	$\approx \dfrac{c}{2B}$
Δv	$= \dfrac{c}{2f_c T_{sym} M}$
R_{max}	$= \dfrac{c T_{cp}}{2}$ (no intersymbol interference)
v_{max}	$= \pm \dfrac{c}{32 f_c T}$ (typical, no intercarrier interference)
ADC rate	$\leq 1\,\text{GHz}$ (typical, I and Q channel)

idea of combining radar and communications [58]–[60], various signal processing improvements [61]–[63] have been presented since then.

An OFDM signal consists of coded signals transmitted on multiple carrier frequencies (called *subcarriers*), continuously and in parallel [Figure 6(d)]. All transmit symbols of all subcarriers are modulated with the same distinct code, for instance, quaternary phase-shift keying, and have a constant symbol length of T_{sym}. To maintain orthogonality, the N subcarriers are uniformly spaced with $\Delta f = 1/T_{sym}$. This results in a total bandwidth of $B = N\Delta f$. Figure 9 shows the spectrum of an OFDM signal with three subcarriers, where the spectrum of each individual subcarrier results in a sinc
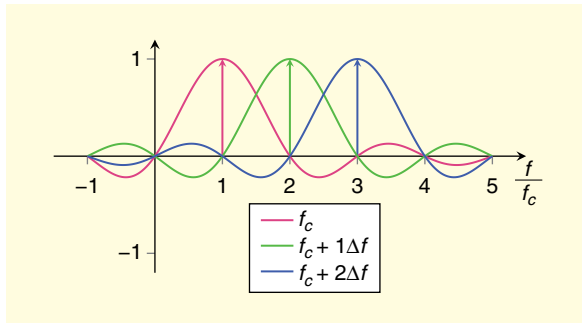
Figure 9. *The spectrum of an OFDM signal with three subcarriers.*

function due to its finite length. Because the carrier spacing is reciprocal to the symbol length, the maximum of every single sinc function is located where all other functions are zero. Therefore, the signals are orthogonal without any intercarrier interference.

The baseband generation of the OFDM signal can be easily realized in the digital domain. The modulation on the individual subcarriers is achieved by applying an inverse fast Fourier transform (IFFT) to all complex symbols $d_{n,m}$ of all $n = 0, \ldots, N-1$ subcarriers for each time instance $m = 0, \ldots, M-1$. A sequence of M OFDM symbols is called a *frame*. To prevent intersymbol interference due to delayed receive signals and multipath effects, each OFDM symbol is extended by a so-called cyclic prefix (CP). The CP is a cyclic repetition of each signal that is added at the beginning of each symbol using a copy of length T_{cp} of the symbol tail. The digital baseband signal is converted from digital to analog, modulated to the carrier frequency, and transmitted through the antenna. After reception, the signal is downconverted to baseband and then digitized. Next, the CP is removed, and the modulation on the subcarriers is reversed using an FFT. In communications, the receive symbols are identified and evaluated in the next step. For radar applications, the channel information $D(n, m)$ is obtained by removing the known baseband transmit symbols from the baseband receive signal. Applying an IFFT along the different subcarriers n and an FFT along subsequent symbols m, the joint range and Doppler information of all targets are extracted from D, yielding an actual 2D range–velocity profile, quite similar to the chirp-sequence evaluation. As in the chirp sequence, the range resolution is directly proportional to the channel bandwidth B, which is equal to the baseband bandwidth in OFDM. The Doppler resolution depends on the total observation time. The maximum unambiguous range depends on the symbol time and the unambiguous Doppler on the carrier spacing, which is also directly linked to the symbol time.

The large baseband bandwidth has the drawback that a large bandwidth must be filtered and sampled at the receiver. Because such hardware is expensive and hard to realize, only a fraction of the required bandwidth is achievable with reasonable effort, making it unusable for automotive applications as the range resolution would not meet the requirements. A solution is to use a narrower bandwidth that is realizable with low-cost hardware and to regain the full resolution of the wider RF bandwidth using different carrier frequencies in a single frame and applying suitable signal postprocessing [64]–[66]. The different discrete carrier frequencies can be realized in a stepped fashion to cover the full channel bandwidth per measurement cycle. Through such a carrier scheme, a full resolution radar image can be obtained at the receiver that has the same range and Doppler resolution as the conventional OFDM signal with wide bandwidth (Figure 10).

Another advantage of OFDM becomes apparent in a MIMO-OFDM radar: multiple transmitters can be employed simultaneously as long as no subcarrier is used by two transmitters at once. To distribute the subcarriers to the transmitters, spectral interleaving is applied [67], [68]. In the case of P transmit antennas, every Pth subcarrier is assigned to one antenna. This guarantees that the individual transmit signals do not interfere but rather use the same bandwidth, which is approximately equal to the baseband bandwidth of an equivalent OFDM signal without interleaving. Maintaining the bandwidth does not result in a reduction of the range resolution; however, sharing carriers reduces the maximum unambiguous range by the number of transmitters.
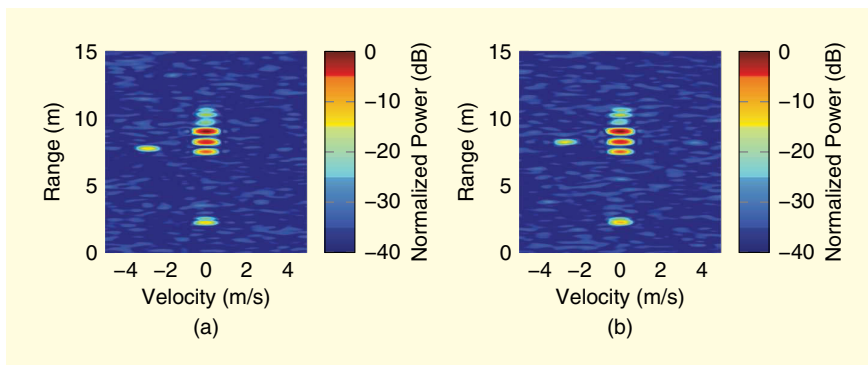

Figure 10. *Two graphs showing 77-GHz OFDM radar measurements with 1-GHz RF bandwidth. In (a), the full baseband bandwidth of 1 GHz is used (high-resolution reference with 1.024 GHz). In (b), only 128-MHz baseband bandwidth is used (eight frequency steps with 128 MHz each). The same RF bandwidth and range resolution are reached using proper signal processing. Figure taken from [64].*

Interference Between Automotive Radars for Different Modulation Schemes

Automated driving applications have challenging requirements for modulation bandwidth, observation time, and update rates. Additionally, an environment perception of 360° in azimuth and the application of height estimation are desired. These demands mean that each car will require multiple radar sensors transmitting to and receiving from surrounding vehicles. If many cars are equipped with a multitude of radar sensors for driver-assistance systems, there is a high probability that the sensors will interfere with each other or even with stationary radars integrated into the infrastructure used for traffic monitoring. Such interference is an important issue with respect to sensor robustness, as it can reduce detection capability or lead to false targets. The problem is especially critical in dense traffic situations.

To underline the significance of the problem, the receive power of an object in distance R given by the radar equation

$$P_R = \frac{P_T G_T G_R \lambda^2 \sigma}{(4\pi)^3 R^4} \qquad (1)$$

is compared with the Friis equation for an interference source in the same distance:

$$P_{\text{int}} = \frac{P_T G_T G_R \lambda^2}{(4\pi)^2 R^2}. \qquad (2)$$

It is assumed that the transmit power P_T, the antenna gain G_T, and the wavelength λ of the interfered with and the interfering sensor are of the same order of magnitude. The receive antenna gain G_R in both (1) and (2) is related to the sensor interfered with. Comparing (1) and (2), the receive power of the targets decreases with R^4, while the interference power decreases only proportional to R^2. Thus, the problem is even more critical for distant objects. Based on (1) and (2), [69] shows that the power level of a target with a radar cross section (RCS) of $1\,\text{m}^2$ at a 200-m distance is about 56 dB below the interference power received from the same distance.

Because of the interference problem, sensors need sufficient countermeasures for reliable functionality in interference situations. The effects and the probability of interference strongly depend on the modulation format. The chance of interference between two FMCW radars depends on multiple factors: the transmit frequencies, transmission times, and ramp slopes determining the duration, as well as how frequently the two radars are operating near each other. While short spikes affecting a few samples in the time signal will be the most common effect in such a setup, leading to a wide-band noise increase in the spectrum [69]–[71], the probability of frequent and long-acting interference is

small—for identical modulation parameters, it is below 10^{-3} [70] for a single measurement.

When interference between chirp-sequence-, PN-, or OFDM-modulated radars is considered, the problem is much more critical. The PN- and OFDM-formats occupy more available spectrum during a measurement cycle and have higher receiver bandwidths. When even more sensors operate at the same time in the 76–77- or 77–81-GHz frequency bands, interference is unavoidable.

FMCW and Chirp-Sequence Interference

The interference between an FMCW and a chirp-sequence radar is depicted in Figure 11. The FMCW ramp regularly intersects the fast frequency chirps, and each time mutual interference occurs. Various investigations [69], [72] showed that this kind of interference adds time-limited, wide-band distortion in the baseband [Figure 11(b)]. The time limitation originates from the antialiasing low-pass filter in the receiver; its bandwidth is indicated in the upper part of the figure. Because of the large ramp slopes and the resulting high baseband frequencies, the filter bandwidth is much wider for chirp-sequence-modulated radars than it is for FMCW-modulated radars.

Figure 11(c) compares the interfered with and interference-free spectrum of the depicted signal. The increased noise level is especially critical for reliable detection of targets with a low RCS, like bicycles or pedestrians. Experiments in [73] show an increased noise level of up to 20 dB in an FMCW radar experiencing interference from a CW radar at a distance of 10 m.

OFDM and PN Interference

The high occupancy of modulation bandwidth over time and the wide receiver bandwidth in the range of several megahertz in chirp-sequence radars lead to increased interference risk compared to slow-ramp FMCW radars. This effect is even more relevant for wide-band OFDM and PN modulation schemes. The receiver bandwidth covers all OFDM carriers during the whole measurement duration. Instead of the time-limited interference in Figure 11, ubiquitous disturbance is present.

Interference between linear, frequency-modulated and wide-band, OFDM-modulated radars also leads to an increased overall noise level in both system types [74], [75]. While an OFDM signal is affected by the full FMCW or chirp-sequence signal power, a linear, frequency-modulated radar is disturbed by only that part of the OFDM signal that falls into the receiver bandwidth B_{Rx} (Figure 12). The interference power in the FMCW or chirp-sequence receiver is proportional to the area indicated by the gray parallelograms in Figure 12 [75].

In PN radars, the interference effects are expected to be similar to those of OFDM-modulated radars. The large receiver bandwidth leads to the reception of a

considerable amount of interference power during the whole measurement time. As long as the interference is uncorrelated to the code sequence, it will result in an increase in wide-band noise.

How Can We Handle the Interference Threat?

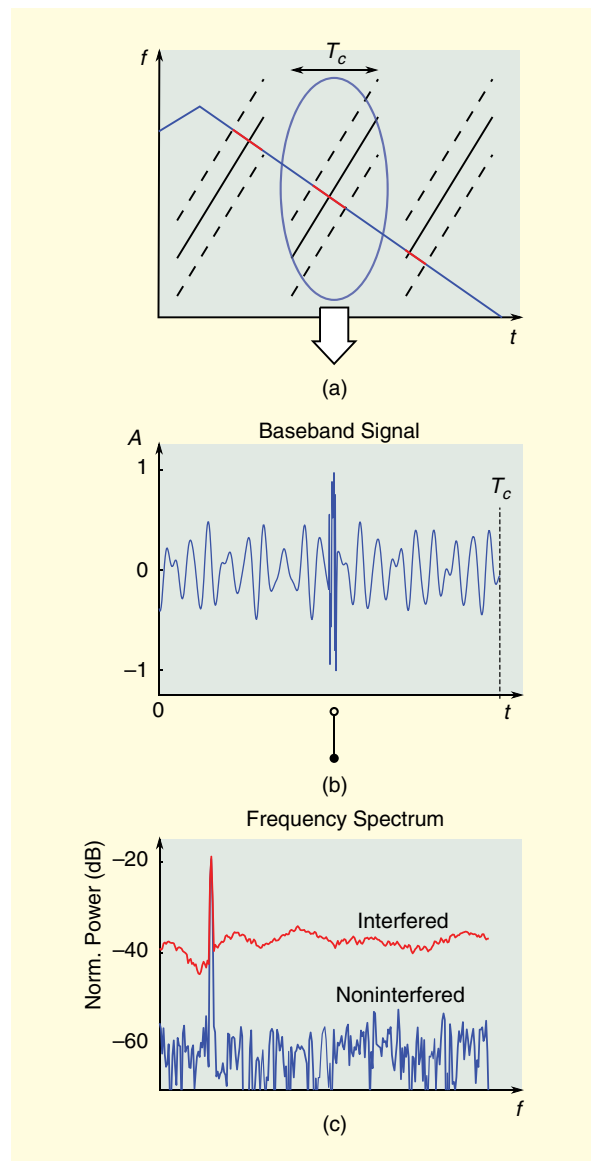Interference as described can severely degrade the performance of radar sensors. To mitigate such effects,

Figure 11. *Graphs showing how an FMCW-modulated radar and a chirp-sequence modulated radar operate in the same frequency band. (a) Interference (red line) occurs in the chirp radar as long as the FMCW signal falls into the receiver bandwidth (broken lines). (b) Time-limited wide-band distortion in the baseband. (c) A comparison of the interfered with and interference-free spectrum of the depicted signal. In the baseband frequency spectrum, the noise floor is raised compared to an interference-free frequency ramp.*

the interference can be detected, and then countermeasures can be applied.

Interference Detection

To detect interference between FMCW or chirp-sequence radars, several detection algorithms have been developed for the time-domain signals. This is done based on the high power and the short duration of the interference in [76]. Other approaches apply matched signal transforms [77] or image-processing methods [78] to detect interference. It was shown that OFDM interference is very difficult to distinguish from thermal noise in the spectrum of FMCW receivers, making detection more problematic [79]. For OFDM radars, a detection algorithm similar to the previously discussed power detectors in combination with an ordered statistic approach is demonstrated in [80].

Time-Domain Approaches

After the detection of the interfered with samples in the time-domain data of chirp-sequence signals, those samples can be set to zero to prevent an increased noise level in the frequency spectrum [69]. However, zeroing requires robust detection and raises additional frequency components; these artifacts can be reduced by introducing a window function at the time-domain discontinuities [78] or a prediction of the missing data with autoregressive models [81]. It is also possible to estimate and afterward cancel the interference component [82] from the time signals. This does not suppress the interference completely, but it does not introduce artifacts in the spectrum.

These time-domain approaches are well-suited for time-limited interference between linear, frequency-modulated radars; however, they are not yet tested for interference from and between code- and OFDM-modulated radars. Code and OFDM modulations occupy a wide bandwidth during the whole duration of a measurement and therefore cause and experience long interference durations. Nevertheless, [80] shows that the data interfered with can be removed and subsequently
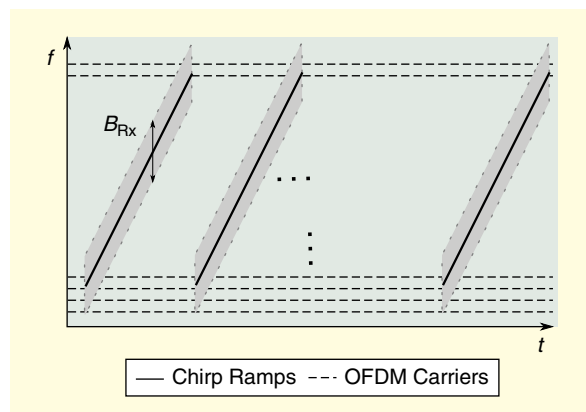

Figure 12. *The interference between an OFDM-modulated and a chirp-sequence-modulated radar. B_{Rx}: receiver bandwidth.*

reconstructed through compressed sensing algorithms when interference among multiple OFDM radars occurs.

Frequency Diversity

As long as the frequency band is not yet completely occupied, frequency hopping can be used for interference mitigation independent of the modulation scheme. However, frequency hopping cannot recover the data of measurements already corrupted by interference. A simple implementation of frequency hopping varies the carrier frequency after each transmission with a pseudorandom selection scheme. As shown with FMCW radars [83], this already leads to a very low probability of permanent interference between two sensors. However, there is a high probability that interference occurs in several measurements.

Another approach suited for chirp-sequence radars is an estimation of an interfering radar's transmit frequency based on the detected interference in the time-domain signals [84]. The high number of chirps in each single measurement leads to a robust estimation followed by adaptive frequency hopping to avoid interference in subsequent measurements. This is suited even more for code and OFDM modulations: their wide receiver bandwidth "scans" the modulation bandwidth during the full measurement duration.

If interfering sensors occupy too much bandwidth, interference-free operation might not be possible in a given frequency band. Even in this scenario, adaptive frequency hopping can align the sensors' bandwidths with the smallest possible overlap (Figure 13). In this case, the window function applied in the signal processing of linear, frequency-modulated radars leads to good interference suppression [72]. The same windowing method is also valid for OFDM radars.

Spatial Masking of Interference Sources

In radar systems with multiple receive channels, it is possible to apply receiver-side digital beamforming (DBF) to suppress signals from an interferer's direction. This direction can be estimated based on the interfered with samples of the time signals [77], [85]. Based on this knowledge, the interference is removed from the field of view (Figure 14), and the desired directions of arrival can be amplified. The opportunities of DBF increase with an increasing aperture size and number of receive channels. Although MIMO radars offer a large virtual aperture size, this virtual aperture cannot be used to suppress interference. The interference affects only the physical receive array and not the whole virtual aperture. Therefore, interference can be canceled only within the physical receive aperture [86].

Interference suppression by DBF is very promising because it is independent of the modulation format of the interfered with and the interfering sensors. It is also not required to detect all interfered with samples in the time signals, as long as the direction of the interfering signals can be determined. However, desired signals in the direction of the interference can no longer be detected. Experimental results for a chirp-sequence system with only four receive channels already show an interference suppression of up to 15 dB [85].

There is one special issue concerning DBF in linear, frequency-modulated radars. As these systems typically do not have an I-Q receiver, the interference energy is spread over multiple directions of arrival because of the interfering signal's image frequency [86]. In this case, a beamformer must consider multiple directions when forming its beams.
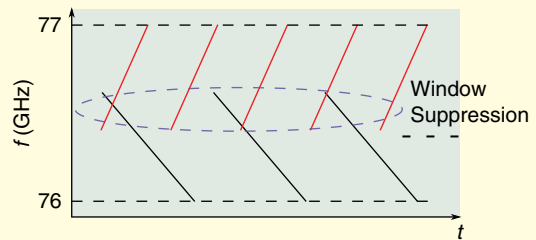

Figure 13. *A graph illustrating what happens when frequency regulations limit the capabilities of frequency hopping. The window function still offers good interference suppression, at least for OFDM and chirp-sequence radars.*
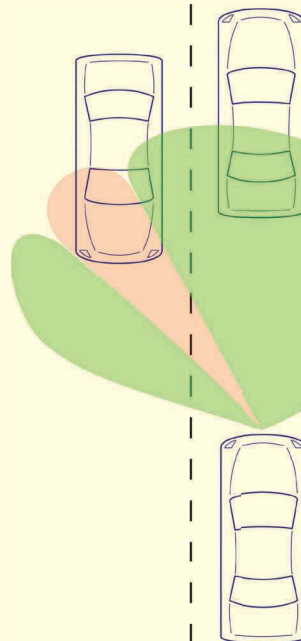

Figure 14. *An illustration of how a beamformer removes the interfering sensor from the field of view.*

Summary

High-Resolution Capabilities

To enable the detection and classification of vulnerable road users in automotive environments, the high-resolution and separability of close targets are key requirements. The lack of any real multitarget capability in the slow FMCW modulation format is a disadvantage. The enhancement of the FMCW scheme, so-called chirp-sequence modulation, has higher but manageable hardware demands and is therefore the current state-of-the-art approach. To enhance the angular resolution, MIMO schemes are used, which could be realized more easily with digital modulation formats.

Demand for Low-Cost Hardware and Efficient Use of Resources

Considering the signal generation and sampling of the resulting baseband signal, slow FMCW has the lowest hardware demands. Transmitting faster-frequency chirps and sampling higher baseband signals are possible at low cost. Hence, the chirp-sequence modulation format is the current state-of-the-art modulation format and has manageable hardware demands.

Both digital modulation formats, PN and OFDM, require, in the basic scheme, a digital-to-analog converter for the signal generation as well as an ADC with full modulation bandwidth. These digital modulation formats, unlike FMCW and chirp-sequence formats, do not offer the advantage of mixing the transmit with the receive signal to gain a low-frequency baseband signal. As this bandwidth is mostly in the range of a couple of gigahertz, either such converters are not available, or the hardware costs are too high for automotive applications. One solution might be to apply stepped OFDM modulations.

Robustness Against Interference

The sensor requirements for automated and autonomous driving make interference an important topic. For FMCW and chirp-sequence modulation, interference will not occur during the whole measurement duration, as the baseband bandwidth is much narrower compared to the transmitted bandwidth. This clearly reduces the chance of collecting interference power from other sensors when compared to both digital modulation formats, where the full transmit bandwidth is sampled during the whole measurement duration. It also reduces the chance of transmitting interfering power into other sensors.

A multitude of methods is available to counteract interference. Time-domain approaches range from calculating power-intensive interpolations of corrupted data to the simple zeroing of interfered with samples. They are most effective for short-duration interference and require reliable detection algorithms. Their specific realization depends on the modulation format. Frequency hopping is very cost-effective in terms of implementation and calculation effort and can offer good performance for interference mitigation. It is, however, limited by the available bandwidth, especially in dense traffic situations with many sensors operating simultaneously. DBF is effective for all modulation schemes, and it does not require detection of all interfered with samples. While suppressing interference, DBF can also amplify directions of interest. On the other hand, the sensor will always be blind toward the direction of the interferer. Furthermore, the performance is limited by the available aperture.

It is not yet clear what kind of interference countermeasures or mitigation approaches are best for the different modulation schemes. It seems reasonable to assume that time-domain approaches are helpful in cases of short interference durations, for example, between linear, frequency-modulated sensors. However, time-domain approaches will experience long interference durations caused by PN- or OFDM-modulated radars. Currently, only a few automotive interference evaluations are available for these radars. Further investigations are required to examine which additional effects might have to be considered and which approach handles interference best.

Conclusions

Autonomous driving has a tremendous influence on the requirements of radar sensors. Different common modulation formats are introduced and compared regarding the new requirements. To establish 360° coverage of the environment, a single radar sensor is not sufficient. This means that each car will need multiple sensors, and, with an increasing number of vehicles on the road, each with multiple sensors, the probability of interference increases. The overview of interference mitigation schemes shows that there are many approaches for making radar operation reliable in multisensor scenarios. Once numerous sensors are operating at the same time, one single approach will not be sufficient. To guarantee reliable operation for all scenarios, multiple interference countermeasures must be combined.

References

[1] Society of Automobile Engineers International, "Taxonomy and definitions for terms related to driving automation systems for on-road motor vehicles," 2016. [Online]. Available: http://standards .sae.org/j3016_201609/

[2] J. Dickmann et al., "Automotive radar the key technology for autonomous driving: From detection and ranging to environmental understanding," in *Proc. IEEE Radar Conf. (RadarConf)*, May 2016. doi: 10.1109/RADAR.2016.7485214.

[3] J. Dickmann et al., "Radar contribution to highly automated driving," in *Proc. European Radar Conf.*, Oct. 2014, pp. 412–415.

[4] H. Buddendick and T. F. Eibert, "Incoherent scattering-center representations and parameterizations for automobiles," *IEEE Antennas Propag. Mag.*, vol. 54, no. 1, pp. 140–148, Feb. 2012.

[5] M. Bühren and B. Yang, "Automotive radar target list simulation based on reflection center representation of objects," in *Proc. Workshop Intelligent Transportation (WIT)*, Hamburg, Germany, Mar. 2006, pp. 161–166.

[6] M. Andres, P. Feil, and W. Menzel, "3D-scattering center detection of automotive targets using 77 GHz UWB radar sensors," in *Proc. European Conf. Antennas and Propagation (EUCAP)*, Mar. 2012, pp. 3690–3693.

[7] M. Andres, W. Menzel, H.-L. Bloecher, and J. Dickmann, "Detection of slow moving targets using automotive radar sensors," in *Proc. German Microwave Conf. (GeMiC)*, Mar. 2012, pp. 1–4.

[8] C. Fischer, H. L. Bloecher, W. Menzel, M. Andres, and J. Dickmann, "Adaptive super-resolution with a synthetic aperture antenna," in *Proc. 9th European Radar Conf. (EuRAD)*, Oct. 2012, pp. 250–253.

[9] S. Olbrich and C. Waldschmidt, "New pre-estimation algorithm for FMCW radar systems using the matrix pencil method," in *Proc. European Radar Conf. (EuRAD)*, Sept. 2015, pp. 177–180.

[10] International Telecommunication Union. (2016). *"Final acts WRC-15: World Radiocommunication Conference (Geneva, 2015),"* Geneva, Switzerland. [Online]. https://www.itu.int/dms_pub/itu-r/opb/act/R-ACT-WRC.12-2015-PDF-E.pdf

[11] *European Telecommunications Standards Institute Short Range Devices; Transport and Traffic Telematics (TTT); Short Range Radar Equipment Operating in the 77 GHz to 81 GHz Band; Harmonised Standard Covering the Essential Requirements of Article 3.2 of Directive 2014/53/EU,* ETSI EN 302 264, 2017.

[12] Federal Communications Commission. (2017). FCC-CIRC1707-07. Washington, DC. [Online]. Available: https://docs.fcc.gov/public/attachments/DOC-345476A1.pdf

[13] Bundesnetzagentur. (2014). Allgemeinzuteilung von Frequenzen für Kraftfahrzeug - Kurzstreckenradare im Frequenzbereich 77–81 GHz. Bonn, Germany. [Online]. Available: https://www.bundesnetzagentur.de/SharedDocs/Downloads/DE/Sachgebiete/Telekommunikation/Unternehmen_Institutionen/Frequenzen/Allgemeinzuteilungen/2004_59_KfzKurzstreckenradar79GHz_pdf.pdf?__blob=publicationFile&v=6

[14] Bundesnetzagentur. (2012). Allgemeinzuteilung von Frequenzen für Kraftfahrzeug-Kurzstreckenradare im Frequenzbereich 21,65–26,65 GHz. Bonn, Germany. [Online]. Available: https://www.bundesnetzagentur.de/SharedDocs/Downloads/DE/Sachgebiete/Telekommunikation/Unternehmen_Institutionen/Frequenzen/Allgemeinzuteilungen/2012_41_KfzKurzstreckenradar24GHz_pdf.pdf?__blob=publicationFile&v=3

[15] F. Roos, J. Klappstein, K. Dietmayer, D. Kellner, J. Dickmann, and C. Waldschmidt, "Estimation of the orientation of vehicles in high-resolution radar images," in *Proc. IEEE MTT-S Int. Conf. Microwaves for Intelligent Mobility (ICMIM)*, Apr. 2015. doi: 10.1109/ICIM.2015.7117949.

[16] F. Roos, D. Kellner, J. Dickmann, and C. Waldschmidt, "Reliable orientation estimation of vehicles in high-resolution radar images," *IEEE Trans. Microw. Theory Techn.*, vol. 64, no. 9, pp. 2986–2993, Sept. 2016.

[17] D. Kellner, M. Barjenbruch, J. Klappstein, J. Dickmann, and K. Dietmayer, "Tracking of extended objects with high-resolution Doppler radar," *IEEE Trans. Intell. Transp. Syst.*, vol. 17, no. 5, pp. 1341–1353, Dec. 2016.

[18] J. Dickmann et al., "Making Bertha see even more: Radar contribution," *IEEE Access*, vol. 3, pp. 1233–1247, 2015.

[19] D. Belgiovane and C.-C. Chen, "Bicycles and human riders Backscattering at 77 GHz for automotive radar," in *Proc. European Conf. Antennas and Propagation (EuCAP)*, Apr. 2016. doi: 10.1109/EuCAP.2016.7481649.

[20] V. C. Chen, F. Li, S.-S. Ho, and H. Wechsler, "Micro-Doppler effect in radar: Phenomenon, model, and simulation study," *IEEE Trans. Aerosp. Electron. Syst.*, vol. 42, no. 1, pp. 2–21, Jan. 2006.

[21] E. Schubert, F. Meinl, M. Kunert, and W. Menzel, "High resolution automotive radar measurements of vulnerable road users—Pedestrians & cyclists," in *Proc. IEEE MTT-S Int. Conf. Microwaves for Intelligent Mobility (ICMIM)*, Apr. 2015. doi: 10.1109/ICMIM.2015.7117944.

[22] D. Kellner, M. Barjenbruch, J. Klappstein, J. Dickmann, and K. Dietmayer, "Instantaneous ego-motion estimation using Doppler radar," in *Proc. Int. IEEE Conf. Intelligent Transportation Systems (ITSC)*, Oct. 2013, pp. 869–874.

[23] D. Kellner, M. Barjenbruch, J. Klappstein, J. Dickmann, and K. Dietmayer, "Instantaneous ego-motion estimation using multiple Doppler radars," in *Proc. IEEE Int. Conf. Robotics and Automation (ICRA)*, May 2014, pp. 1592–1597.

[24] K. Werber, J. Klappstein, J. Dickmann, and C. Waldschmidt, "Interesting areas in radar gridmaps for vehicle self-localization," in *Proc. IEEE MTT-S Int. Conf. Microwaves for Intelligent Mobility (ICMIM)*, May 2016. doi: 10.1109/ICMIM.2016.7533932.

[25] J. Ziegler et al. "Making Bertha drive—An autonomous journey on a historic route," *IEEE Intell. Transp. Syst. Mag.*, vol. 6, no. 2, pp. 8–20, 2014.

[26] P. Häcker and B. Yang, "Single snapshot DOA estimation," *Advances Radio Sci.*, vol. 8, pp. 251–256, 2010. [Online]. Available: http://www.adv-radio-sci.net/8/251/2010/

[27] R. O. Schmidt, "Multiple emitter location and signal parameter estimation," *IEEE Trans. Antennas Propag.*, vol. 34, no. 3, pp. 276–280, Mar. 1986.

[28] P. Stoica and K. C. Sharman, "Maximum likelihood methods for direction-of-arrival estimation," *IEEE Trans. on Acoust., Speech, and Signal Processing*, vol. 38, no. 7, pp. 1132–1143, July 1990.

[29] M. Schoor and B. Yang, "High-resolution angle estimation for an automotive FMCW radar sensor," in *Proc. Int. Radar Symp. (IRS)*, 2007, pp. 1–5.

[30] Robert Bosch GmbH, "LRR3: 3rd generation long-range radar sensor." 2009. [Online]. Available: http://products.bosch-mobility-solutions.com/media/db_application/downloads/pdf/safety_1/en_4/lrr3_datenblatt_de_2009.pdf

[31] A. Stove, "Linear FMCW radar techniques," *IEE Proc. F—Radar Signal Processing*, vol. 139, no. 5, pp. 343–350, Oct. 1992.

[32] V. Winkler, "Range Doppler detection for automotive FMCW radars," in *Proc. 4th European Radar Conf. (EuRAD)*, Oct. 2007, pp. 166–169.

[33] C. Schroeder and H. Rohling, "X-band FMCW radar system with variable chirp duration," in *Proc. IEEE Radar Conf.*, May 2010, pp. 1255–1259.

[34] F. Roos, M. Barjenbruch, N. Appenrodt, J. Dickmann, and C. Waldschmidt, "Enhancement of Doppler resolution for chirp-sequence modulated radars," in *Proc. European Radar Conf. (EuRAD)*, Oct. 2016, pp. 237–240.

[35] K. Thurn, D. Schmakov, G. Li, S. Max, M.-M. Meinecke, and M. Vossiek, "A novel interlaced chirp sequence radar concept with range-Doppler processing for automotive applications," in *Proc. IEEE MTT-S Int. Microwave Symp. (IMS)*, May 2015. doi: 10.1109/MWSYM.2015.7166715.

[36] K. Thurn, D. Schmakov, G. Li, S. Max, M.-M. Meinecke, and M. Vossiek, "Concept and implementation of a PLL-controlled interlaced chirp sequence radar for optimized range-Doppler measurements," *IEEE Trans. Microw. Theory Techn.*, vol. 64, no. 10, pp. 3280–3289, Oct. 2016.

[37] J. J. M. de Wit, W. L. van Rossum, and A. J. de Jong, "Orthogonal waveforms for FMCW MIMO radar," in *Proc. IEEE RadarCon (RADAR)*, May 2011, pp. 686–691.

[38] H. Sun, F. Brigui, and M. Lesturgie, "Analysis and comparison of MIMO radar waveforms," in *Proc. Int. Radar Conf.*, Oct. 2014. doi: 10.1109/RADAR.2014.7060251.

[39] C. M. Schmid, R. Feger, C. Pfeffer, and A. Stelzer, "Motion compensation and efficient array design for TDMA FMCW MIMO radar systems," in *Proc. 6th European Conf. Antennas and Propagation (EUCAP)*, Mar. 2012, pp. 1746–1750.

[40] J. Bechter, F. Roos, and C. Waldschmidt, "Compensation of motion-induced phase errors in TDM MIMO radars," *IEEE Microw. Compon. Lett.*, vol. 27, no. 12, pp. 1164–1166, Dec. 2017.

[41] R. Feger, H. Haderer, and A. Stelzer, "Optimization of codes and weighting functions for binary phase-coded FMCW MIMO radars," in *Proc. IEEE MTT-S Int. Conf. Microwaves for Intelligent Mobility (ICMIM)*, May 2016. doi: 10.1109/ICMIM.2016.7533916.

[42] W. Van Thillo, P. Gioffré, V. Giannini, D. Guermandi, S. Brebels, and A. Bourdoux, "Almost perfect auto-correlation sequences for binary phase-modulated continuous wave radar," in *Proc. European Radar Conf.*, Oct. 2013, pp. 491–494.

[43] A. Bourdoux, U. Ahmad, D. Guermandi, S. Brebels, A. Dewilde, and W. Van Thillo, "PMCW waveform and MIMO technique for a 79 GHz CMOS automotive radar," in *Proc. IEEE Radar Conf. (RadarConf)*, May 2016. doi: 10.1109/RADAR.2016.7485114.

[44] A. Vazquez, M. G. Sanchez, I. Cuinas, and M. Dawood, "Wideband noise radar based in phase coded sequences." in *Radar Technology*, G. Kouemou, Ed. London: Intech, 2010.

[45] V. Giannini et al., "A 79 GHz phase-modulated 4 GHz GHz-BW CW radar transmitter in 28 nm CMOS," *IEEE J. Solid-State Circuits*, vol. 49, no. 12, pp. 2925–2937, Dec. 2014.

[46] D. Guermandi et al., "A 79 GHz binary phase-modulated continuous-wave radar transceiver with TX-to-RX spillover cancellation in 28 nm CMOS," in *Proc. IEEE Int. Solid-State Circuits Conf.*, Feb. 2015. doi: 10.1109/ISSCC.2015.7063072.

[47] K. Kobayashi, T. Morita, H. Mukai, T. Kishigami, and Y. Nakagawa, "79 GHz-band coded pulse compression radar system performance in outdoor for pedestrian detection," in *Proc. European Radar Conf.*, Oct. 2013, pp. 327–330.

[48] W. Van Thillo, V. Giannini, D. Guermandi, S. Brebels, and A. Bourdoux., "Impact of ADC clipping and quantization on phase-modulated 79 GHz CMOS radar," in *Proc. 11th European Radar Conf.*, Oct. 2014, pp. 285–288.

[49] W. Menzel, J. Buechler, and J. Taech, "An experimental 24 GHz radar using phase modulation spread spectrum techniques," in *Proc. 28th European Microwave Conf.*, Oct. 1998, vol. 2, pp. 56–60.

[50] V. Filimon and J. Buechler, "A pre-crash radar sensor system based on pseudo-noise coding," in *Proc. IEEE MTT-S Int. Microwave Symp. Dig.*, June 2000, vol. 3, pp. 1415–1418.

[51] H. J. Ng, R. Feger, and A. Stelzer, "A fully-integrated 77-GHz pseudo-random noise coded Doppler radar sensor with programmable sequence generators in SiGe technology," in *Proc. IEEE MTT-S Int. Microwave Symp.*, June 2014. doi: 10.1109/MWSYM.2014.6848382.

[52] R. Feger, H. Haderer, H. J. Ng, and A. Stelzer, "Realization of a sliding-correlator-based continuous-wave pseudorandom binary phase-coded radar operating in W-band," *IEEE Trans. Microw. Theory Techn.*, vol. 64, no. 10, pp. 3302–3318, Oct. 2016.

[53] H. Haderer, R. Feger, C. Pfeffer, and A. Stelzer, "Millimeter-wave phase-coded CW MIMO radar using zero- and low-correlation-zone sequence sets," *IEEE Trans. Microw. Theory Techn.*, vol. 64, no. 12, pp. 4312–4323, Dec. 2016.

[54] T. Hwang, C. Yang, G. Wu, S. Li, G. Y. Li, "OFDM and its wireless applications: A survey," *IEEE Trans. Veh. Technol.*, vol. 58, no. 4, pp. 1673–1694, May 2009.

[55] R. W. Chang, "Synthesis of band-limited orthogonal signals for multichannel data transmission," *Bell Syst. Tech. J.*, vol. 45, no. 10, pp. 1775–1796, 1966.

[56] S. B. Weinstein and P. M. Ebert, "Data transmission by frequency-division multiplexing using the discrete Fourier transform," *IEEE Trans. Commun. Technol.*, vol. 19, no. 5, pp. 628–634, 1971.

[57] N. Levanon, "Multifrequency complementary phase-coded radar signal," *IEE Proc.—Radar, Sonar Navigation*, vol. 147, no. 6, pp. 276–284, Dec. 2000.

[58] B. J. Donnet and I. D. Longstaff, "Combining MIMO radar with OFDM communications," in *Proc. 3rd European Radar Conf.*, 2007, pp. 37–40.

[59] D. Garmatyuk, J. Schuerger, and K. Kauffman, "Multifunctional software-defined radar sensor and data communication system," *IEEE Sensors J.*, vol. 11, no. 1, pp. 99–106, Jan. 2011.

[60] C. Sturm and W. Wiesbeck," Waveform design and signal processing aspects for fusion of wireless communications and radar sensing," in *Proc. IEEE*, 2011, vol. 99, no. 7, pp. 1236–1259.

[61] R. F. Tigrek, W. J. A. De Heij, and P. Van Genderen," Multi-carrier radar waveform schemes for range and Doppler processing," in *Proc. IEEE Nat. Radar Conf.*, 2009, pp. 2–6.

[62] C. R. Berger, B. Demissie, J. Heckenbach, P. Willett, and S. Zhou, "Signal processing for passive radar using OFDM waveforms," *IEEE J. Sel. Topics Signal Process.*, vol. 4, no. 1, pp. 226–238, Feb. 2010.

[63] C. Sturm, E. Pancera, T. Zwick, and W. Wiesbeck, "A novel approach to OFDM radar processing," in *Proc. IEEE Nat. Radar Conf.*, 2009, no. 3, pp. 9–12.

[64] B. Schweizer, C. Knill, D. Schindler, and C. Waldschmidt, "Stepped-carrier OFDM-radar processing scheme to retrieve high-resolution range-velocity profile at low sampling rate," *IEEE Trans. Microw. Theory Techn.*, vol. 66, no. 3, pp. 1610–1618, 2017.

[65] G. Lellouch, A. K. Mishra, and M. Inggs, "Stepped OFDM radar technique to resolve range and Doppler simultaneously," *IEEE Trans. Aerosp. Electron. Syst.*, vol. 51, no. 2, pp. 937–950, 2015.

[66] C. Pfeffer, R. Feger, and A. Stelzer, "A stepped-carrier 77-GHz OFDM MIMO radar system with 4 GHz bandwidth," in *Proc. 2015 European Radar Conf. (EuRAD)*, Sept. 2015, pp. 97–100.

[67] Z. Wang, F. Tigrek, O. Krasnov, F. Van Der Zwan, P. Van Genderen, and A. Yarovoy, "Interleaved OFDM radar signals for simultaneous polarimetric measurements," *IEEE Trans. Aerosp. Electron. Syst.*, vol. 48, no. 3, pp. 2085–2099, 2012.

[68] C. Sturm, Y. L. Sit, M. Braun, and T. Zwick, "Spectrally interleaved multi-carrier signals for radar network applications and multi-input multi-output radar," *IET Radar, Sonar Navigation*, vol. 7, no. 3, pp. 261–269, 2013.

[69] G. M. Brooker, "Mutual interference of millimeter-wave radar systems," *IEEE Trans. Electromagn. Compat.*, vol. 49, no. 1, pp. 170–181, Feb. 2007.

[70] D. Oprisan and H. Rohling, "Analysis of mutual interference between automotive radar systems," in *Proc. Int. Radar Symp. (IRS)*, Berlin, 2005, pp. 1–8.

[71] M. Goppelt, H.-L. Blöcher, and W. Menzel, "Automotive radar—Investigation of mutual interference mechanisms," *Advances Radio Sci.*, vol. 8, pp. 55–60, 2010.

[72] T. Schipper, M. Harter, T. Mahler, O. Kern, and T. Zwick, "Discussion of the operating range of frequency modulated radars in the presence of interference," *Int. J. Microwave Wireless Technologies*, vol. 6, pp. 371–378, June 2014.

[73] T. Schipper, T. Mahler, M. Harter, L. Reichardt, and T. Zwick, "An estimation of the operating range for frequency modulated radars in the presence of interference," in *Proc. European Radar Conf. (EuRAD)*, Oct. 2013, pp. 227–230.

[74] G. Hakobyan and B. Yang, "A novel narrowband interference suppression method for OFDM radar," in *Proc. 24th European Signal Processing Conf. (EUSIPCO)*, Aug. 2016, pp. 2230–2234.

[75] C. Knill, J. Bechter, and C. Waldschmidt, "Interference of chirp sequence radars by OFDM radars at 77 GHz," in *Proc. IEEE MTT-S Int. Conf. Microwaves for Intelligent Mobility (ICMIM)*, Mar. 2017, pp. 147–150.

[76] C. Fischer, M. Goppelt, H.-L. Blöcher, and J. Dickmann, "Minimizing interference in automotive radar using digital beamforming," *Advances Radio Sci.*, vol. 9, pp. 45–48, 2011.

[77] C. Fischer, H.-L. Blöcher, J. Dickmann, and W. Menzel, "Robust detection and mitigation of mutual interference in automotive radar," in *Proc. 16th Int. Radar Symp. (IRS)*, June 2015, pp. 143–148.

[78] M. Barjenbruch, D. Kellner, K. Dietmayer, J. Klappstein, and J. Dickmann, "A method for interference cancellation in automotive radar," in *Proc. IEEE MTT-S Int. Conf. Microwaves for Intelligent Mobility (ICMIM)*, Apr. 2015. doi: 10.1109/ICMIM.2015.7117925.

[79] S. Heuel, "Automotive radar interference test," in *Proc. 18th Int. Radar Symp. (IRS)*, June 2017. doi: 10.23919/IRS.2017.8008119.

[80] B. Nuss, L. Sit, and T. Zwick," A novel technique for interference mitigation in OFDM radar using compressed sensing," in *Proc. IEEE MTT-S Int. Conf. Microwaves for Intelligent Mobility (ICMIM)*, Mar. 2017, pp. 143–146.

[81] B. E. Tullsson, "Topics in FMCW radar disturbance suppression," in *Proc. Radar 97*, Oct. 1997. doi: 10.1049/cp:19971620.

[82] J. Bechter, K. D. Biswas, and C. Waldschmidt, "Estimation and cancellation of interferences in automotive radar signals," in *Proc. 18th Int. Radar Symp. (IRS)*, June 2017. doi: 10.23919/IRS.2017.8008126.

[83] L. Mu, T. Xiangqian, S. Ming, and Y. Jun, "Research on key technologies for collision avoidance automotive radar," in *Proc. Intelligent Vehicles Symp.*, June 2009, pp. 233–236.

[84] J. Bechter, C. Sippel, and C. Waldschmidt, "Bats-inspired frequency hopping for mitigation of interference between automotive radars," in *Proc. IEEE MTT-S Int. Conf. Microwaves for Intelligent Mobility (ICMIM)*, May 2016. doi: 10.1109/ICMIM.2016.7533928.

[85] J. Bechter, K. Eid, F. Roos, and C. Waldschmidt, "Digital beamforming to mitigate automotive radar interference," in *Proc. IEEE MTT-S Int. Conf. Microwaves for Intelligent Mobility (ICMIM)*, May 2016. doi: 10.1109/ICMIM.2016.7533914.

[86] J. Bechter, M. Rameez, and C. Waldschmidt, "Analytical and experimental investigations on mitigation of interference in a DBF MIMO radar," *IEEE Trans. Microw. Theory Techn.*, vol. 65, no. 5, pp. 1727–1734, May 2017.